Kybernetika

Jiří Krýže; A. Krýžová; Roman Mikoláš; M. Salaba

System dynamics identification by means of adjustable models

Kybernetika, Vol. 2 (1966), No. 6, (508)--530

Persistent URL: http://dml.cz/dmlcz/125710

Terms of use:

© Institute of Information Theory and Automation AS CR, 1966

Institute of Mathematics of the Academy of Sciences of the Czech Republic provides access to digitized documents strictly for personal use. Each copy of any part of this document must contain these *Terms of use*.

This paper has been digitized, optimized for electronic delivery and stamped with digital signature within the project *DML-CZ: The Czech Digital Mathematics Library* http://project.dml.cz

KYBERNETIKA ČÍSLO 6, ROČNÍK 2/1966

System Dynamics Identification by means of Adjustable Models

J. KRÝŽE, A. KRÝŽOVÁ, R. MIKOLÁŠ, M. SALABA

Two methods for system dynamics identification based on processing of recorded stochastic input and output signals of a system by means of adjustable models were thoroughly experimentally tested on a laboratory scale.

The theoretical discussion of the methods involved and results obtained yields insight into the advantageous properties and intrinsic limitations of straightforward model methods.

1. INTRODUCTION

Among other methods for identifying dynamic parameters of control systems, the methods based on knowledge of input and output signals of general stochastic character seem to raise a rising interest in the last time. Blandhol [1] and Norkin [2] showed in their papers some new possibilities of the model method.

The authors of the reported work decided to investigate experimentally on a laboratory scale some of the possible modifications of the model methods using the specialized computer MUSA 6 [3, 4, 5] which is able to record and reproduce very exactly comparatively long intervals of input and output signals of some system.

The main interest was in parameter identification of systems which, for technological or economical reasons, permit an analysis based on stochastic signals recorded during normal operation only.

The basic methodology of the experiment was therefore chosen similar to that described in [1]:

First, the signal from a generator of stochastic processes G (fig. 1) was connected to the input of a system S. The transfer function of this system was supposed to be of the form

$$F_\sigma(p) = \frac{\beta_0 + \beta_1 p + \ldots + \beta_n p^n}{\alpha_0 + \alpha_1 p + \ldots + \alpha_n p^n} = \frac{M_\sigma(p)}{N_\sigma(p)} \tag{1}$$

where $M_\sigma(p)$ and $N_\sigma(p)$ denote the polynomials of the nominator and denominator, respectively.

The input signal x_1 and the output signal x_2 were recorded in the memory MM.

When analysed, the signals x_1 and x_2 were reproduced and fed into a model M formed on an analog computer (fig. 2).

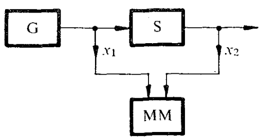

Fig. 1. Recording of signals.

On the model coeficients a_i and b_i were set by hand so as to minimize the mean square value K of the deviation Δ:

(2) $$K = \frac{1}{T}\int_0^T \Delta^2(t)\,\mathrm{d}t$$

which was used as the criterion for the quality of approximation of the values α_i and β_i (now supposed to be unknown) by the values a_i and b_i, respectively.

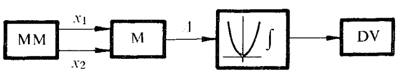

Fig. 2. Anylysis of recorded signals.

For each setting of a_i and b_i the whole recorded data for x_1 and x_2 were reproduced at least once; according to the obtained value of the criterion K, indicated on a digital voltmeter DV, a new setting of a_i and b_i was chosen.

2. METHODS USED FOR FORMING THE DEVIATION SIGNAL Δ

One of the most straightforward methods for this purpose is illustrated in fig. 3. On the model the transfer function

(3) $$F_s(p) = \frac{b_0 + b_1 p + \ldots + b_n p^n}{a_0 + a_1 p + \ldots + a_n p^n} = \frac{M_s(p)}{N_s(p)}$$

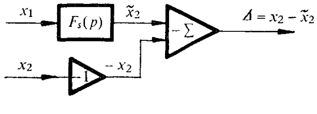

Fig. 3. Basic scheme of the ITF method.

is formed. The Laplace transform of the deviation signal is then

$$\Delta(p) = X_1(p)[F_\sigma(p) - F_s(p)] . \tag{4}$$

In [2] a new identification method is suggested and theoretically motivated. The structure in fig. 4 is based on the general principles used in this method for forming

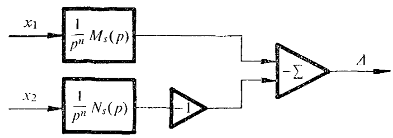

Fig. 4. Basic scheme of the DTF method.

the deviation signal Δ. Here

$$\Delta(p) = X_2(p)\frac{1}{p^n}N_s(p) - X_1(p)\frac{1}{p^n}M_s(p) = \tag{5}$$

$$= X_1(p)\frac{1}{p^n}[N_s(p)F_\sigma(p) - M_s(p)] ,$$

$$\Delta(p) = X_1(p)[F_\sigma(p) - F_s(p)]\frac{N_s(p)}{p^n} . \tag{6}$$

The transfer functions $N_s(p)/p^n$ and $M_s(p)/p^n$ consist of pure integrations. This would in practice inevitably lead to instability caused by DC unbalance, and drifts and a steady increase of Δ limited only by amplifier saturation would be the result. In [2] this difficulty is overcome by postulating values of integration constants in each of a number of successive integration steps which ensure the mean value of the involved functions to be the same after integration as before.

This postulate was not respected quite exactly, because otherwise a rather complex scheme would be necessary. But a fairly good approximation was used. This was achieved by a change in the transfer functions $N_s(p)/p^n$ and $M_s(p)/p^n$ ensuring insensitivity of the method to the values of integration constants by suppression of the lowest part of the frequency band used. As a rule this part is, of almost no interest for identification purposes.

We can, therefore, use a high-pass filter with a transfer function $F_H(p)$ and choose a sufficiently low limiting frequency so that the interesting part of the Δ spectrum is left unchanged.

Then, instead of the transfer functions $N_s(p)/p^n$ and $M_s(p)/p^n$ the transfer functions

$$\frac{N_s(p)}{p^n} F_H(p) \quad \text{and} \quad \frac{M_s(p)}{p^n} F_H(p) \tag{7}$$

are used, where the high-pass filter transfer function

$$F_H(p) = \frac{p^m}{p^m + \sum_{i=1}^{m} c_i p^{m-i}} \tag{8}$$

is formed so as to secure minimum deviation from 1 above the chosen limiting frequency.

Both transfer functions in (7) are then realizable by conventional analog computer techniques without difficulties, because the zero poles in (7) are cancelled by zeroes of (8); the denominator of $F_H(p)$ must, of course, be stable.

Then, there results the deviation signal Δ:

$$\Delta(p) = X_1(p)[F_\sigma(p) - F_s(p)] \frac{N_s(p)}{p^n} F_H(p) . \tag{9}$$

This method in accordance with fig. 4 will be referred to as the Distributed Transfer Function Method (DTF), whereas the first one will be referred to as the Integrated Transfer Function Method (ITF) for distinction.

The DFT method has some advantageous features which cannot be found in the ITF method. The most important one is the mutual orthogonality of settings of coefficients a_i with even and odd potences of p in the $N_s(p)$ transfer function. By this orthogonality, proved in [2], the independence of the value a_i defined by

$$\frac{\partial K}{\partial a_i} = 0 \tag{10}$$

on the settings of all values a_{i+2k+1} (k is an integer) is understood. A similar independence of the values b_i defined by

$$\frac{\partial K}{\partial b_i} = 0 \tag{11}$$

on the settings of all values b_{i+2k+1} can be found both in the DTF and the ITF methods.

Comparison of the expressions (6) and (9) for $\Delta(p)$ in both methods shows that the signal Δ for DTF can be gained from the signal Δ in ITF by adding a filter with the transfer function

$$\frac{N_s(p)}{p^n} F_H(p) .$$

The transfer function $N_s(p)/p^n$ depends on a_i settings. It is this dependence which is responsible for the orthogonality of settings of coefficients a_i with odd and even indexes.

The absolute value of $N_s(p)/p^n$ is, however, always greater on the lower end of the used spectral band than on the upper end. The addition of the transfer function $N_s(p)/p^n$ results therefore in a relative suppression of higher frequencies. This can hardly be considered an advantage, because it makes more defficult to recognize details of the system transfer function in the higher frequency region which, as a rule, is the most important region for control purposes.

One of the main tasks of the experiment which was carried out in November 1965 in the Institute of Information Theory and Automation of the Czechoslovak Academy of Sciences, in collaboration with Mr. V. D. Spiridonov from the Institute of Automation and Telemechanics of the Academy of Sciences of the USSR, according to an agreement between the mentioned Institutes, was the verification and the comparison of the features of both methods.

3. METHODOLOGY OF THE EXPERIMENT

For simulation of the system and for creating adjustable models, a small analog computer MEDA (described in [6]) was used. There was no substantial departure from conventional

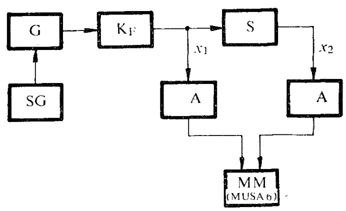

Fig. 5. Recording apparatus (A — amplifier).

feedback analog computer programming techniques and it seems therefore unnecessary to show the used schemes in detail.

The block diagram for recording the signals x_1 and x_2 into the memory is shown in fig 5. The input random signal x_1 was obtained by filtering of a telegraph random signal by the filter K_F. The telegraph random signal was delivered by the generator G of the random process GENAP, described in [17] which was controlled by a signal generator SG. The shape of the autocorrelation function of this signal is shown in fig. 6 where Θ is equal to the basic interval of the telegraph signal. For the described measurements $\Theta = 0{\cdot}5$ ms was chosen.

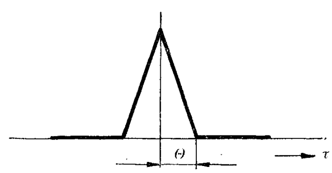

Fig. 6. Autocorrelation function of random signal generator output.

The signal x_1 should have a spectral density similar to spectral densities expected to be found in x_1 signals in field applications. These will be generally falling with increasing frequency.

Therefore, an integrating network was chosen for the filter K_F with the transfer function $1/(1 + \tau_F p)$. Its time constant τ_F was made equal to the highest time constant of the system S.

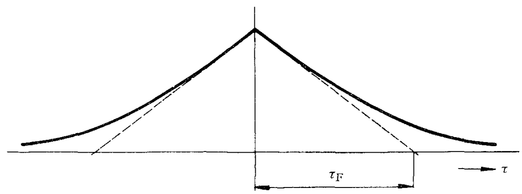

Fig. 7. Autocorrelation function of $x_1(t)$.

With the examinated system transfer functions its numerical volue was

$$\tau_F = 100 \text{ ms} .$$

Because $\tau_F \gg \Theta$, the autocorrelation function of the input noise x_1 has a nearly exponential form (see fig. 7) with the time constant τ_F.

A desirable frequency response $|F_H(j\omega)|$ of general form is shown in fig. 8. A high-pass filter

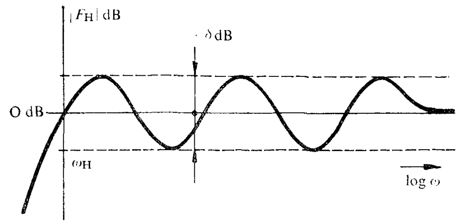

Fig. 8. Filter frequency response F_H, generally.

of the second order with the amplitude frequency response shown in fig. 9 and the transfer function

$$F_H(p) = \frac{p_2}{p_2 + 6{,}132p + 27{,}47} \tag{13}$$

was used in the experiment.

To the basic schemes shown in fig. 2, 3 and 4 several further elements were added, as indicated in fig. 10.

Differentiating networks with time constants τ_1 and τ_2 were used to remove direct current components arising by high amplification of drift and zero unbalance of D.C. amplifiers. Since differentiating networks are high-pass filters, the same conclusions are valid for their use as for the high-pass filter $F_H(p)$.

The MUSA 6, used as a magnetic tape memory, repeats periodically the recorded signals x_1 and x_2 during the identification process. Every time a play back of the signals is started or finished, transient processes in the used models and filters are generated. These transients are caused by abrupt changes in the recorded x_1 and x_2 signals on the beginning and end of their recording.

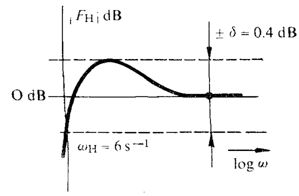

Fig. 9. Frequency response F_H of filter, as used.

The influence of these transients is suppressed by the key k. This key closes only after a time, necessary for full decay of transients, has elapsed from the beginning of x_1 and x_2 recordings; it opens just before their end. Then the signal Δ obtained does not differ from the signal Δ which would be obtained with infinitely long records.

The useful part of x_1 and x_2 processes, that is, the part not suppressed by k, was represented by some 35 000 values of each of the variables.

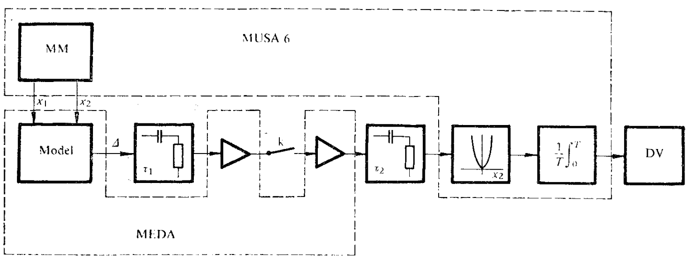

Fig. 10. Basic scheme used for identification ($\tau_1 = 165$ msec used for ITF and $\tau_1 = \infty$ for DTF; $\tau_2 = 1{\cdot}6$ sec).

4. HYPERSURFACE FORMS

The criterion K, established and measured in accordance with (2) and the methods described, is a function of the settings of the coefficients a_i and b_i, and it depends also on the signal and gain levels used.

To exclude this last mentioned dependence, and to get results of a more general meaning, a dimensionless measure of K was introduced:

(14) $$\varkappa = \frac{K}{K_T}$$

where

(15) $$K_T = \frac{1}{T}\int_0^T \Delta_T^2 \, dt \, .$$

Here Δ_T denotes the deviation signal Δ for the correct setting of a_i and b_i, but with the x_1 or x_2 path in fig. 10 disconnected. The form of the hypersurfaces defined by

(16) $$\varkappa = f(a_i, b_i) = \text{const}$$

is of great interest from the identification standpoint.

The function

(17) $$\varkappa = f(a_i, b_i)$$

can be in the neighbourhood of the optimum approximated by a quadratic form; as will be shown by the experimental results, this approximation is fairly good for surprisingly great deviations of a_i and b_i from their optimal values.

Denoting the relative deviations of a_i and b_i from their optimal values a_{i0} and b_{i0} by

(18) $$\delta_i = \frac{a_i - a_{i0}}{a_{i0}}, \quad 0 \leqq i \leqq n \, ,$$

(19) $$\delta_{n+i} = \frac{b_i - b_{i0}}{b_{i0}}, \quad 0 < i \leqq n$$

(b_0 is supposed to be choosen as the constant coefficient) one can write the approximation of (17) as follows:

(20) $$\varkappa = \sum_{i,k=0}^{i,k=2n} \lambda_{ik}\delta_i\delta_k \, ,$$

The measurement was carried out especially for two cases:

a) only one δ_i is set to a chosen value, all other δ_k, where $k \neq i$, being left zero: For this case (20) yields:

(21) $$\varkappa = \lambda_{ii}\delta_i^2 \, ;$$

b) one δ_i is set to a chosen value, alle other δ_k, where $k \neq i$, being adjusted to minimize $\varkappa$:

(22) $$\frac{\partial \varkappa}{\partial \delta_k} = 0 \quad \text{for} \quad k \neq i \, .$$

 Then (21) yields

$$\varkappa = \mu_i \delta_i^2 \tag{23}$$

where

$$\mu_i = \frac{M}{M_{ii}}. \tag{24}$$

In (24) M denotes the determinant of the matrix $\|\lambda_{ik}\|$ and M_{ii} is the subdeterminant for the element λ_{ii}. The changes in δ_k are related to the change in δ_i by

$$\delta_k = \frac{M_{ik}}{M_{ii}} \delta_i = \mu_{ik} \delta_i . \tag{25}$$

The values

$$\alpha_{ik} = \frac{M_{ik}}{M} = \frac{\mu_{ik}}{\mu_i}, \quad \alpha_{ii} = \frac{M_{ii}}{M} = \frac{1}{\mu_i} \tag{26}$$

which can be evaluated from the measured values of $\varkappa, \delta_i$ and δ_k according to (23), (24) and (25), form a symmetrical matrix. The matrices $\|\lambda_{ik}\|$ and $\|\alpha_{ik}\|$ are related by the equation

$$\|\alpha_{ik}\| \cdot \|\lambda_{ik}\| = 1 \tag{27}$$

and hence values of $\|\lambda_{ik}\|$ can be computed from measured values $\|\alpha_{ik}\|$, or vice versa.

The axes of the hyperellipsoid corresponding to (20) are determined by the eigenvalues λ of the matrix $\|\lambda_{ik}\|$. For a given $\varkappa$ the length of an axis is equal to $\sqrt{(\varkappa/\lambda)}$ and its direction is given by the respective eigenvector.

5. NOISE INFLUENCE

Let us consider a field application of the mentioned model methods where the studied system is noisy. This situation is illustrated in fig. 11. Besides the input signal x_1

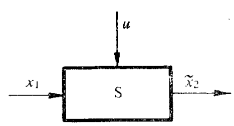

Fig. 11. Noise influence on x_2.

also a noise u enters the system, causing the output to consist of two components:

$$\tilde{x}_2 = x_2 + v \tag{28}$$

where x_2 is due to the input x_1 and related to it by the transfer function $F_a(p)$ and v is due to the noise u. Both the noise and the transfer function relating v to u are supposed to be unknown.

For the ITF method the signal Δ influenced by noise will be

(29) $$\tilde{\Delta} = \Delta + v .$$

Let us suppose that u and x_1 are statistically independent. Then for the criterion we get:

(30) $$\tilde{K} = \frac{1}{T}\int_0^T \tilde{\Delta}^2 \, dt \doteq \frac{1}{T}\int_0^T (\Delta^2 + v^2) \, dt$$

because due to statistical independence of x_1 and u also v and x_1, v and x_2, and hence, v and Δ are statistically independent. The mean value of the $\Delta \,.\, v$ product tends, therefore, to zero if T is increased sufficiently

(31) $$\lim_{T\to\infty} \frac{1}{T}\int_0^T \Delta \,.\, v \, dt = 0 .$$

Thus,

(32) $$\tilde{K} = K + \tilde{K}_{\min}$$

where $\tilde{K}_{\min}$ is the value of $\tilde{K}$ for optimum setting of a_i and b_i, that is for $\Delta = 0$:

(33) $$\tilde{K}_{\min} = \frac{1}{T}\int_0^T v^2 \, dt .$$

It can be seen from (32) that a minimum of $\tilde{K}$ occurs, if K is minimal (zero), because $\tilde{K}_{\min}$ is a constant. No change in the minimum position will be caused by the disturbing noise u, and the same a_i and b_i values should result.

But this is not exactly the case, bacause the values of K gained from the scheme on fig. 10 are never quite accurate. They are influenced by errors, due partly to the simplifications used (finitness of recording intervals, supposition of system linearity) and partly to apparatus imperfectness (e.g. drifts, model nonlinearity, gain variations, external noises).

As a result of these errors the correct value of $\tilde{K}$ can be measured only with some uncertainty the relative value of which in neighbourhood of the minimum of $\tilde{K}$ is designated by ϑ.

The minimal significant change in $\tilde{K}$ will then be equal to the absolute value of this uncertainty:

(34) $$(\Delta\tilde{K})_{\min} = K = \vartheta \tilde{K}_{\min} .$$

Such change in $\tilde{K}$ has to be produced by the minimal discernible deviation from optimum in settings of the coefficients a_i and b_i. For the ITF method

(35) $$\Delta_T = x_2$$

so that (15) yields

(36) $$K_T = \frac{1}{T}\int_0^T x_2^2 \, \mathrm{d}t \, .$$

The RMS signal to noise ration η in the $\tilde{x}_2$ signal is then given by

(37) $$\eta^2 = \frac{K_T}{\tilde{K}_{\min}}$$

and for the minimal significant change in $\tilde{K}$ from (34) one gets an expression for the minimal significant change in $\varkappa$:

(38) $$\varkappa = \frac{\vartheta}{\eta^2} \, .$$

Combining (38) and (23) one gets

$$\delta_i = \frac{1}{\eta}\sqrt{\frac{\vartheta}{\mu_i}}$$

which determines the maximal relative error in a_i setting to be expected in the presence of a disturbing noise. In a similar way, the length of the longest axis of the hyperellipsoid for the $\varkappa$ value defined by (38):

(40) $$\delta_T = \frac{1}{\eta}\sqrt{\frac{\vartheta}{\lambda_{\min}}}$$

is the length of the maximum error vector

(41) $$\delta_T = \sqrt{\left(\sum_i \delta_i^2\right)} \, .$$

Thus, the sensitivity coefficients λ_{ik} and μ_i and the eigenvalues λ are very important figures of merit, showing directly the limits imposed on the examined methods by noise and apparatus imperfectness. The values μ_{ik} allow to estimate the mutual interference of individual coefficient setting in the optimization process; for an ideal orthogonality all μ_{ik}, $i \neq k$, would be zero.

The analysis for the DFT method has to take into account the additive filtering action on the deviation signal defined by (12). Signals $\tilde{x}_2$ and $\tilde{v}$, gained from x_2 and v by filtering through a filter (12), have to be substituted for x_2 and v in (29), (30), (31) and (33).

The value $\tilde{K}_{\min}$ then depends on a_i settings, because the transfer function (12) and hence $\bar{v}$ are dependent on these settings.

Consequently, the position of the minimum of $\tilde{K}$ differs from the position of the minimum of K generally, the change in individual coefficients being a complex function of the signal to noise ratio, x_2 and v spectral density forms and α_i and β_i values. The exact analysis of this function exceeds the scope of this paper.

But it may be noted that the analysis of noise influence derived for the ITF method applies also to the DTF method in the special case where only noise generated in the computing machinery, independent on a_i and b_i settings, can be considered as responsible for the $\tilde{K}_{\min}$ value.

6. THE RESULTS

Systems with four transfer functions were simulated and then both DTF and ITF identification methods were applied to the recorded signals. The used transfer functions were as follows:

a) A simple first order transfer function

$$F_\sigma(p) = \frac{1}{1 + 0{,}1p}. \tag{42}$$

b) A simple second order transfer function without numerator and with real roots:

$$F_\sigma(p) = \frac{1}{1 + (4/30)p + (1/300)p^2} = \frac{300}{(p + 10)(p + 30)}. \tag{43}$$

c) A simple second order transfer function without numerator and with complex roots:

$$F_\sigma(p) = \frac{1}{1 + (p/10)\sqrt{(2)} + (p^2/100)} = \frac{100}{[p + 5\sqrt{(2)}(1 + j)][p + 5\sqrt{(2)}(1 - j)]}. \tag{44}$$

d) A second order transfer function with a first order numerator and real roots:

$$F_\sigma(p) = \frac{1 + p/20}{1 + (4/30)p + (p^2/300)} = \frac{15(p + 20)}{(p + 10)(p + 30)}. \tag{45}$$

For a), b), c) a detailed measurement, consisting of several hundred points, of the κ function (17) was taken allowing to construct the hypersurfaces $\kappa = \text{const}$. For the simplest case a) the system of these hypersurfaces is reduced to a system of contour lines $\kappa = \text{const}$. in the $\delta_0 - \delta_1$ plane. For b) and c) the equation $\kappa = \text{const}$. describes conventional three-dimensional surfaces. An idea about the overall form of these surfaces can be drawn from the three normal cross-sections formed by contour lines in the three normal planes, defined by the δ_0 and δ_1, δ_1 and δ_2, δ_2 and δ_0 pairs of axes. These sections are shown in figs 12 to 15.

From figs 12 to 15 it is quite apparent that the approximation of the κ function (17) by the quadratic form (20) is fairly good for δ_i to some 10%–20% and for κ to $64 . 10^{-4}$. This can be seen from the very nearly elliptic form of the contour lines and from the very nearly linear scales formed on any line passing through the origin by interceptions with the system of contour lines corresponding to a quadratic scale of κ values.

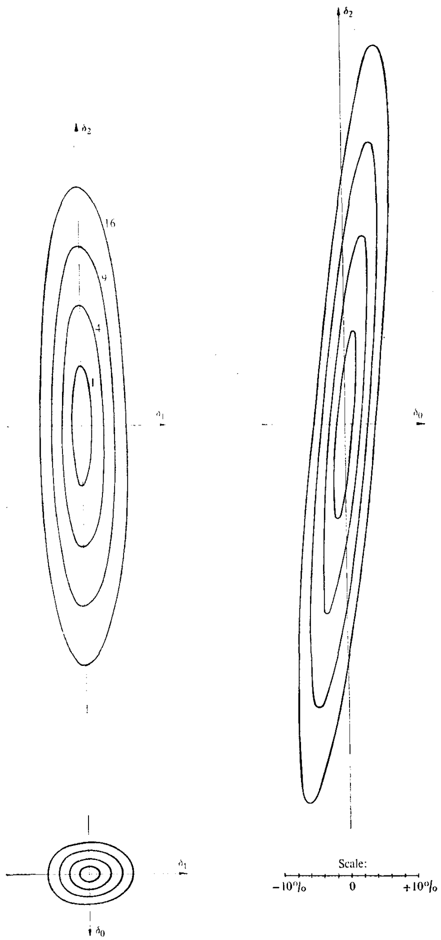

Fig. 12. Contour lines gained by three normal sections through the system of surfaces κ = const. = (1, 4, 9, 16) . 10^{-4} for the second order transfer function with real roots and DTF method.

The measurements taken showed that also for δ_i twice (and κ four times) as great as shown in figs 12 to 15 the departure from the quadratic form is not very significant.

No secondary minima were found in any of the reported cases; thus it can be concluded that the hypersurfaces in both identification methods seem to have a fairly simple, nearly quadratic form in a wide neighbourhood of the optimal settings of a_i and b_i coefficients.

This would be no doubt very advantageous for automation of the identification procedure. The only, but very significant remaining trouble arises from the possibility of very lengthy elliptic

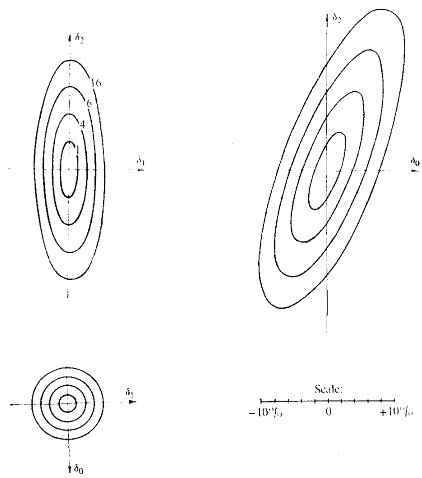

Fig. 13. Same as fig. 12, but ITF method.

(or generally hyperellipsoidal) forms with considerable inclination to coordinate system axes. As illustrated by fig. 16 in such a case finite probe steps in all four directions from point P can lead to a false conclusion that P is a minimum. Therefore taking account of this possibility, some more elaborate optimizing method has to be used.

In some of the figures, especially figs. 14 and 15, there is a slight, but noticeable departure from the orthogonality of odd and even coeffcients. The reason for this discrepancy with the orthogonality theory could lie, theoretically, in a short lenght of the recorded processes. But with the number of samples used a substantial deviation from the asymptotic values has a low probability. Another explanation seems more likely, that is, model imperfectness. With the used frequency band ranging to 2 kHz the small machine MEDA worked well on the top of its possibilities with respect to frequency response. Additional phase shifts and parasitic capacitive couplings may cause several other coefficients of the transfer function to be slightly influenced by the change of the element value (e.g. potenciometer setting) corresponding to any given coefficient. In a first approximation the effect of this is a linear transformation of coordinate axes comprising shifts and rotations.

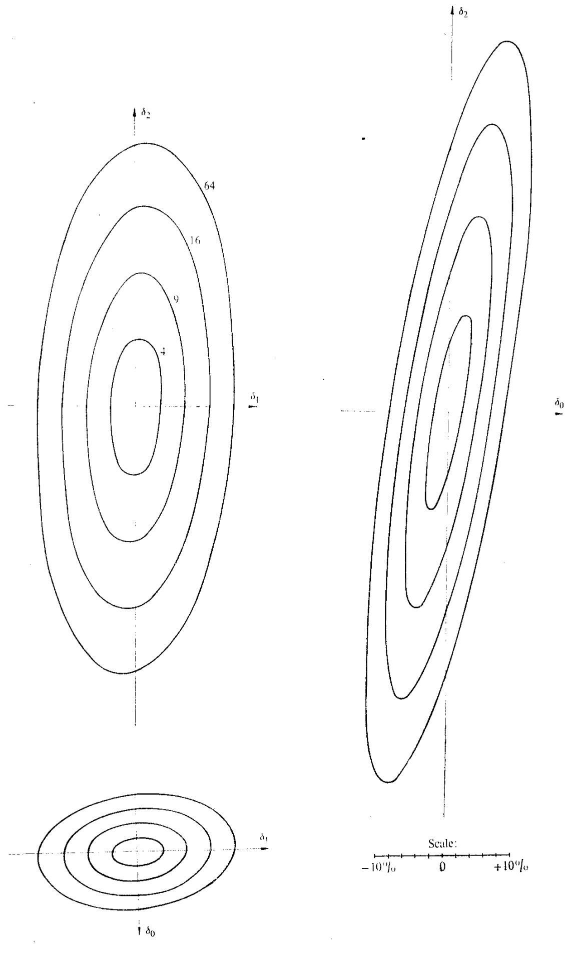

Fig. 14. Contour lines gained by three normal sections through the system of surfaces $\kappa = \text{const.} = (4, 16, 36, 64) \cdot 10^{-4}$ for the second order transfer function with complex roots and DTF method.

Respecting this observation, and noticing that there is no noticeable change in the inclination of ellipses when κ is increased, one may conclude that no substantial difference, concerning orthogonality of odd and even coefficients, can be observed in the DTF and ITF method, though theory guarahtees this orthogonality for the DTF method generally and for the ITF method only for the optimal setting.

For the last case d), the detailed measurement which should consist of at least six normal sections was not made. Nevertherless, sufficient points were taken to confirm the applicability of the quadratic approximation (20).

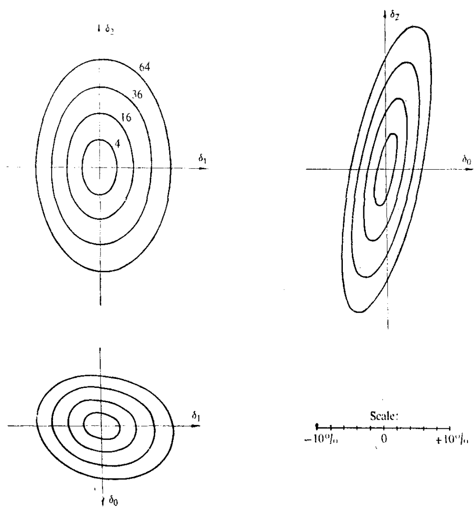

Fig. 15. Same as fig. 14, but ITF method.

The quantitative discussion can be more readily made from the $\|\alpha_{ik}\|$ and $\|\lambda_{ik}\|$ matrix values and axis lengths and positions. These are shown in tables 1, 2 and 3. The vectors of axes shown in these tables are shown for $\kappa = 1$, and their absolute value is thus given by the respective eigenvalue:

(46)
$$\delta_{\text{abs}} = \sqrt{\frac{1}{\lambda}}.$$

Equation (37) may then be rewritten as:

(47)
$$\delta_T = \frac{\delta_{\text{absmax}}}{\eta} \sqrt{\vartheta}\,.$$

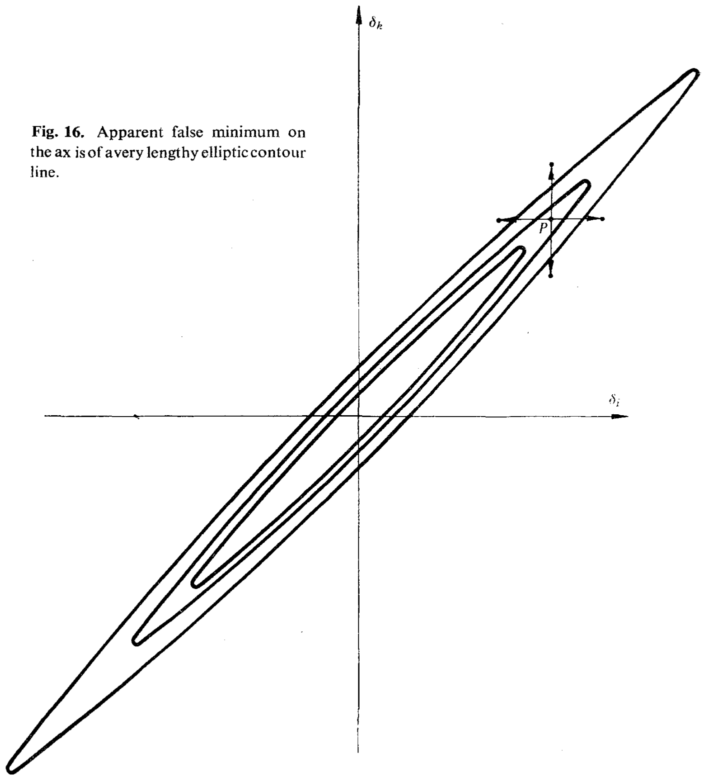

Fig. 16. Apparent false minimum on the ax is of a very lengthy elliptic contour line.

Taking $\vartheta = 0{\cdot}01$ and $\eta = 10$ as arbitrary values, representing a rough estimate of very favourable conditions in field application of the methods described, one gets

(48) $$\delta_T = 0{\cdot}01\delta_{\text{absmax}} = \delta_{\text{absmax}}\%$$

and the column δ_{abs} in tables 1, 2, 3 can be regarded as total identification error expressed in percents and expected with signal to noise ratio 10 and method and apparatus inaccuracy of finding $\tilde{K}\,\vartheta = 1\%$.

From this standpoint the results for the first order transfer function shown in table 1 can be regarded as encouraging both for the small absolute value of δ_{abs} and for orthogonality of δ_0 and δ_1.

Table 1.

Matrices for First Order Transfer Function

Method	$\|\alpha_{ik}\|$		$\|\lambda_{ik}\|$		$\|\lambda_{ik}\|$	Vectors of axes		
						δ_0	δ_1	δ_{abs}
DTF	1·21	0	0·826	0	0·464	0	1·4	1·4
	0	1·96	0	0·511		1·1	0	1·1
ITF	1·56	0	0·64	0	0·2415	0	1·62	1·62
	0	2·64	0	0·379		1·25	0	1·25

Unfortunately, the picture changes substantially if the order of the transfer function is raised by a single unit. The longest axis grows very rapidly, in one case as much as ten times. Also the ratio of longest to shortest axis increases approximately in the same proportions.

The ITF method is here substantially better than the DTF method, giving approximately a 2·5 times shorter longest axis and a 2 or 3 times smaller ratio of longest to shortest axes. Also the inclination of the longest axis is less with the ITF method.

A quite similar difference exists between the results for real and complex roots for any of the methods.

The explanation can be easily found by spectral density considerations. The used noise, due to its autocorrelation function form, has a spectral density function falling 100 times for a decade of frequency change over $\omega = 10$. Moreover, the system itself damps the higher frequencies substantially. For the DTF method, when compared with the ITF method, a further damping of high frequencies, expressed by the additive filter (12), takes place.

It is obvious that such changes in the transfer function of the model which affect the high frequency part of the respective frequency response only will under the described circumstances affect only a small part of the total noise energy, that is, their impact on κ will be hardly noticeable.

Therefore, the transfer function with real roots having one root substantially farther in the high frequency region, and the DTF method having more damping of high frequency components, yield poorer results in this case.

Unfortunately, the high frequency part of a frequency response characteristic is, as a rule the most interesting part for control applications. The input noise spectrum, the falling character of which is one of the sources of troubles, will hardly have a better composition in field applications.

The matrices in table 2 were computed from λ_{ik} values computed from axes positions of the ellipses in figs. 12 to 15. The matrix $\|\lambda_{ik}\|$ was then inverted and checked with the $\|\alpha_{ik}\|$ values gained from measured μ_i and μ_{ik} values. There were no troubles with the sensitivity of the inversion process to experimental inacuracies of λ_{ik} values and a good agreement was reached.

Of course, some of the $\|\lambda_{ik}\|$ and $\|\alpha_{ik}\|$ matrices have nonzero values λ_{01}, λ_{12}, α_{01}, α_{12}, which correspond to the discrepancy with the orthogonality theory mentioned in the discussion of fig. 12 to 15.

The situation with the matrices $\|\alpha_{ik}\|$ in table 3 was worse. Their rows are nearly linearly dependent, indicating a needle form of the hyperellipsoid. The exact values of both $\|\lambda_{ik}\|$ and $\|\alpha_{ik}\|$ matrices could be determined only by a method using the knowledge of diagonal values of both matrices, which are least influenced by measuring errors, and some of the most dependable values of $\|\alpha_{ik}\|$, that is, of the values of which the inacuracy has least influence on the computed values. α_{02} and α_{03} have proved to have this quality. But possible inaccuracies involved by this method have no effect on the δ^2_{abs} max value which is here practically equal to the

Table 2.

Matrices for Second Order Transfer Function, $b_1 = 0$

System and method	$\|\alpha_{ik}\|$			$\|\lambda'_{ik}\|$			$1000 \times \times \|\lambda_{ik}\|$	Vectors of axes			
								δ_0	δ_1	δ_2	δ_{abs}
Real	3·1	0	18	0·73	0	−0·071		1·4	0	13·6	13·7
roots,	0	2·5	0	0	0·39	0	1·55	0	1·59	0	1·59
DTF	18	0	186	−0·071	0	0·012		1·16	0	−0·119	1·16
Real	3·2	−0·06	6·2	0·53	0	−0·11		1·22	−0·056	5·4	5·53
roots,	−0·06	1·82	−0·18	0	0·55	0·0054	9·88	perpendicular plane			1·35
ITF	6·2	−0·28	29	−0·11	0·0054	0·058		to longest axes			1·35
Complex	2·3	−0·08	7·3	0·86	0·051	−0·13		1·09	0·116	6·9	6·98
roots,	−0·08	3·4	0·77	0·051	0·3	−0·0127	5·345	0·167	−1·83	0·0044	1·84
DTF	7·3	0·77	48	−0·13	−0·0127	0·042		1·05	0·095	−0·167	1·07
Complex	1·88	0·33	2·7	1·07	−0·095	−0·036		1·07	0·254	2·77	2·98
roots,	0·33	1·7	0·53	−0·095	0·61	0·0088	82·84	0·129	1·27	−0·167	1·19
ITF	2·7	0·53	7·8	−0·36	−0·0088	0·255		−0·84	0·126	0·313	0·90

Table 3.

Matrices for Second Order Transfer Function, $b_1 \neq 0$

Method	$\|\alpha_{ik}\|$				$\|\lambda_{ik}\|$				$10^6 \|\lambda_{ik}\|$	Vectors of axes				
										δ_0	δ_1	δ_2	δ_3	δ_{abs}
DTF	1·5	0·15	7·6	0·38	0·96	0	−0·063	0·076		0·034	42·5	128	106	1·1
	0·15	1800	5400	4500	0	0·3	0	0·12	0·2413	−0·7	2·04	−4·61	4·75	6·96
	7·6	5400	16300	13500	0·63	0	0·0135	−0·016		0·082	1·55	0·016	−0·64	1·68
	0·38	4500	13500	11300	0·076	−0·12	−0·016	0·068		1·00	−0·016	−0·068	0·088	1·01
ITF	2·9	0·15	3·7	0·39	0·46	0	−0·11	0·13		0·05	14·5	45	38	60·8
	0·15	210	644	547	0	0·625	0	−0·24	14·59	1·2	−0·8	1·6	1·6	2·7
	3·7	644	2060	1700	−0·11	0	0·098	−0·12		1·17	0·54	−0·37	0·23	1·38
	0·39	547	1700	1435	0·13	−0·24	−0·12	0·23		0·3	−0·99	−0·15	0·56	1·18

sum of diagonal values of $\|\alpha_{ik}\|$ which were measured directly

$$\delta^2_{\text{absmax}} \doteq \sum_i \alpha_{ii} \,. \tag{49}$$

The validity of this approximation is based on the high ratio between α_{ii} and λ_{ii} values.

The matrices in table 3 illustrate the interesting fact that orthogonality of odd and even a_i coefficients, expressed by $\lambda_{01} = \lambda_{12} = 0$, does not mean that there is no influence of errors in odd coefficients settings to even coefficients settings found by minimization of κ; on the contrary, from the second row of both $\|\alpha_{ik}\|$ matrices we find

$$\frac{\delta_2}{\delta_1} = \mu_{12} = \frac{\alpha_{12}}{\alpha_{11}} \doteq 3 \tag{50}$$

that is, a 1% error in a_1 setting causes the value a_2 to be found with a 3% error.

This is caused by the interference of b_1 which is orthogonal with no a_i coefficient. A change in a_1 setting causes a shift in the position of b_1 minimum, and the resulting change of b_1 shifts the a_2 minimum.

If the results in table 2 could perhaps appear yet acceptable for a practical application, this could hardly be said about the δ_{abs} values in table 3.

Like in table 2, the ITF method yields here better results. The largest axis and its ratio to the shortest one is approximately three times less if ITF the method is used.

Nevertherless, the results for ITF are not acceptable for practical application.

Together with the spectral situation already discussed one further circumstance is also responsible for the poor results. In the transfer function (45), like in all transfer functions with a numerator there is more room for compensation of a change of one coefficient by changes of others. This compensation can, e.g., limit the influence of a shift of a pole to a short portion of the frequency characteristic, ranging from that pole to the next zero or pole.

But details of the frequency response characteristic which influence only a narrow frequency band will have a very slight effect on the whole spectral energy of the error signal $\tilde{\Delta}$ if disturbing noise is present.

An error in identifying coefficients of a transfer function has to be judged not only by its total value but also by its components, that is, by its direction if it is regarded as a vector. The influence of errors in various coefficients can add or compensate in the control loop. Ideally, a change, which is irrelevant for the control loop, could be allowed to be less noticeable in the identification process. The errors for the transfer function (45) lie nearly always in the direction of the longest axis because the sensitivity in this direction, (that is the change in κ for a given error) compared with the most favourable direction, is 2650 times less for ITF and 28700 times less for DTF. The direction of the longest axis is nearly the same for both ITF and DTF and can be expressed approximately by the ratio

$$\delta_1 : \delta_2 : \delta_3 = 1 : 3 : 2{\cdot}5 \,. \tag{51}$$

Fig. 17 shows the asymptotic logarithmic frequency response characteristics of the transfer function (42) for nominal values (full line) and for $\delta_T = 0{\cdot}5$ in the longest axis direction, that is

$$\delta_1 = 0{\cdot}124 \,; \quad \delta_2 = 0{\cdot}372 \,; \quad \delta_3 = 0{\cdot}31 \,. \tag{52}$$

Fig. 17 proves that the changes of the individual coefficients compensate each other and the resulting effect on the frequency response is much less than that corresponding to an error of the same magnitude in any single coefficient. One may thus expect that also in a control loop the δ_i changes will compensate to a certain extent. An exact estimation is, of course, not possible without some knowledge about the respective control loop.

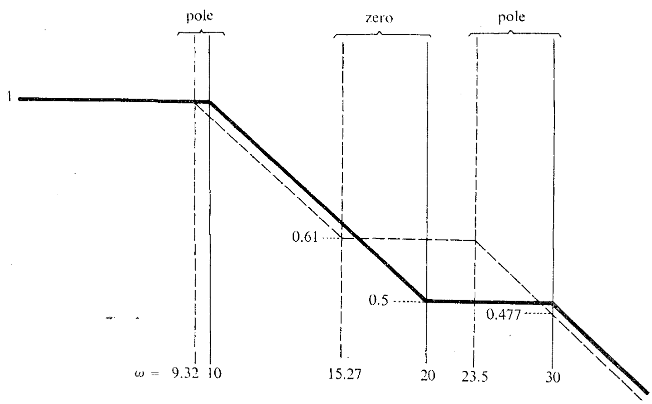

Fig. 17. Effect of total error $\sigma_T = 0{\cdot}5$ in long axis direction on frequency response.

CONCLUSIONS

Both studied methods yield possibilities for automation of the identification process from the standpoint of hypersurface $\varkappa$ = const. form simplicity.

The ITF method proved to be substantially better from the sensitivity standpoint if more than two parameters are to be determined.

The sensitivity of both methods decreases extremely rapidly if the number of unknown parameters is raised. The rate of this decrease in the experiments involved can be very roughly expressed by two orders of magnitude per one unknown parameter added (that is, one order of magnitude of error increase).

Thus, no simple straightforward method seems promising if more than three parameters are unknown, inspite of the favourable circumstance that errors which compensate from the identification method standpoint seem to compensate to a certain extent from the control loop design standpoint too.

The most natural way for improving the method sensitivity seems to be some filtering of the signals involved which would stress the frequencies lying in the band most influenced by the respective coefficient changes and suppressing those which do not.

(Received March 29th, 1966.)

[1] Blandhol E., Balchen I. G.: Determination of System Dynamics by use of Adjustable Models. Automatic and Remote Control — Proc. of the 1963, IFAC Conference in Basle, Vol. 1, pp. 602—614.

[2] Норкин К. В.: Приложение теории среднеквадратичных приближений к линейным самонастраивающимся моделям. Автоматика и телемеханика *XXVI* (1965), 7, 1216—1222.

[3] Krýže J.: An Universal Statistical Analyser. Automatic and Remote Control, Proc. of the IFAC Congress — Basle 1963, Applications and Components, pp. 676—686.

[4] Krýže J.: Methods for Storage and Processing of Analog Data, Used in MUSA-6. Kybernetika *1* (1965), 2, 144—179.

[5] Krýže J.: MUSA - 6 — Ein universeller statistischer Analysator. Zeischrift für Messen, Steuern, Regeln *6* (1963), 7, pp. 286—298 and 9, pp. 386—391.

[6] Škarda J.: Meda, malý elektronický diferenciální analysátor. Sborník V — Stroje na zpracování informací, NČSAV 1957.

[7] Eykhoff P., Smith O. J. M.: Optimalizing Control with Process Dynamics Identification. IRE Transaction on Automatic Control *AC-7* (1962), 140—155.

[8] Schmidt G.: Selfeinstellender Regelkreis mit Bezugsmodell. Regelungstechnik (1962), 4, 145—151.

[9] Reinisch K.: Verwendung eines Modellregelkreises zur Gewinnung einfacher Bemessungsregeln für lineare Regelkreise und zur Ermittlung der Kennwerte von Regelstrecken. Zeitschrift für Messen, Steuern, Regeln u. Automatisierung (1960), No 6, 245—256.

[10] Donalson J., Leondes C. T.: A Model Referenced Parameter Tracking Technic for Adaptive Control Systems. IEEE Transactions on Applications and Industry (1963, September), 241—252.

[11] Weygandt C. N., Puri N. N.: Transfer Function Tracking and Adaptive Control Systems. IRE Transactions Automatic Control *AC-6* (May 1961), 2, 162—166.

[12] Kitamori T.: Applications of Orthogonal Functions to the Determination of Process Dynamic Characteristics and to the Construction of Self-optimizing Control Systems. Automatic and Remote Control, Proc. of the 1960 IFAC Conference in Moscow, vol. II, vol. II, 613—619.

[13] Margolis M., Leondes C. T.: On the Theory of Adaptive Control Systems; the Learning Model Approach. Automatic and Remote Control, Proc. of the 1960 IFAC Conference in Moscow, vol. II, 555—564.

[14] Braun L. Jr., Mishkin E. and Truxal J. G.: Approximate Identification of Process Dynamics in Computer Controlled Adaptive Systems. Automatic and Remote Control, Proc. of the 1960 IFAC Conference in Moscow, vol. II, 596—604.

[15] Gibson J. F.: Self-optimizing or Adaptive Control Systems. Automatic and Remote Control, Proc. of the 1960 IFAC Conference in Moscow, vol. II, 586—596.

[16] Фельдаум А. А.: Автоматический оптимизатор. Автоматика и телемеханика. *XIX* (1958), 8.

[17] Havel J.: An Electronic Generator of Random Sequences. Transactions of the Second Prague Conference on Information Theory, Statistical Decision Functions and Random Processes, 1960, 219—229.

Identifikace dynamických parametrů regulačních soustav pomocí nastavitelných modelů

J. Krýže, A. Krýžová, R. Mikoláš, M. Salaba

V ÚTIA ČSAV byla ve spolupráci s pracovníky IAT AV SSSR provedena s pomocí stroje MUSA-6 podrobná experimentální prověrka dvou metod, užívajících modelů pro identifikaci dynamických parametrů soustav na základě zpracování zaznamenaných vstupních a výstupních signálů stochastického charakteru.

Zejména byl podrobně prověřen vliv odchylek od správného nastavení modelů na hodnotu použitého integrálního kvadratického kritéria, tvar nadploch s konstantní hodnotou tohoto kritéria. Z výsledků jsou odvozovány závěry o možnostech identifikace dynamických parametrů za přítomnosti rušivých šumů a podrobněji osvětleny některé výhodné i limitující faktory v metodách zkoumaného druhu.

Ing. Jiří Krýže, CSc., Ing. Anna Krýžová, Ing. Roman Mikoláš, Ing. Miroslav Salaba, Ústav teorie informace a automatizace ČSAV, Vyšehradská 49, Praha 2.